





OPEN

Drug repositioning in non-small cell lung cancer (NSCLC) using gene co-expression and drug–gene interaction networks analysis

Habib MotieGhader^{1,2}, Parinaz Tabrizi-Nezhadi^{1,2}, Mahshid Deldar Abad Paskeh³, Behzad Baradaran⁴, Ahad Mokhtarzadeh⁴, Mehrdad Hashemi^{3,5}, Hossein Lanjanian⁶, Seyed Mehdi Jazayeri⁷, Masoud Maleki¹, Ehsan Khodadadi⁸, Sajjad Nematzadeh⁹, Farzad Kiani¹⁰, Mazaher Maghsoudloo^{5,11} & Ali Masoudi-Nejad¹¹

Lung cancer is the most common cancer in men and women. This cancer is divided into two main types, namely non-small cell lung cancer (NSCLC) and small cell lung cancer (SCLC). Around 85 to 90 percent of lung cancers are NSCLC. Repositioning potent candidate drugs in NSCLC treatment is one of the important topics in cancer studies. Drug repositioning (DR) or drug repurposing is a method for identifying new therapeutic uses of existing drugs. The current study applies a computational drug repositioning method to identify candidate drugs to treat NSCLC patients. To this end, at first, the transcriptomics profile of NSCLC and healthy (control) samples was obtained from the GEO database with the accession number GSE21933. Then, the gene co-expression network was reconstructed for NSCLC samples using the WGCNA, and two significant purple and magenta gene modules were extracted. Next, a list of transcription factor genes that regulate *purple* and *magenta* modules' genes was extracted from the TRRUST V2.0 online database, and the TF–TG (transcription factors–target genes) network was drawn. Afterward, a list of drugs targeting TF–TG genes was obtained from the DGldb V4.0 database, and two drug–gene interaction networks, including drug–TG and drug–TF, were drawn. After analyzing gene co-expression TF–TG, and drug–gene interaction networks, 16 drugs were selected as potent candidates for NSCLC treatment. Out of 16 selected drugs, nine drugs, namely *Methotrexate*, *Olanzapine*, *Haloperidol*, *Fluorouracil*, *Nifedipine*, *Paclitaxel*, *Verapamil*, *Dexamethasone*, and *Docetaxel*, were chosen from the drug–TG sub-network. In addition, nine drugs, including *Cisplatin*, *Daunorubicin*, *Dexamethasone*, *Methotrexate*, *Hydrocortisone*, *Doxorubicin*, *Azacitidine*, *Vorinostat*, and *Doxorubicin Hydrochloride*, were selected from the drug–TF sub-network. *Methotrexate* and *Dexamethasone* are common in drug–TG and drug–TF sub-networks. In conclusion, this study proposed 16 drugs as potent candidates for NSCLC treatment through analyzing gene co-expression, TF–TG, and drug–gene interaction networks.

Lung cancer is one of the leading cancer death causes¹ worldwide. This type of cancer occurs when a cancerous tumor grows inside the lungs. Lung cancer contains two main types: non-small cell lung cancer (NSCLC) and

¹Department of Biology, Tabriz Branch, Islamic Azad University, Tabriz, Iran. ²Department of Health Ecosystem, Medical Faculty, Nisantasi University, Istanbul, Turkey. ³Farhikhtegan Medical Convergence Sciences Research Center, Farhikhtegan Hospital Tehran Medical Sciences, Islamic Azad University, Tehran, Iran. ⁴Immunology Research Center, Tabriz University of Medical Sciences, Tabriz, Iran. ⁵Department of Genetics, Faculty of Advanced Science and Technology, Tehran Medical Sciences, Islamic Azad University, Tehran, Iran. ⁶Molecular Biology and Genetics Department, Engineering and Natural Science Faculty, Istinye University, Istanbul, Turkey. ⁷Departamento de Biología, Universidad Nacional de Colombia, Bogotá, Colombia. ⁸Department of Agronomy and Plant Breeding, Tabriz Branch, Islamic Azad University, Tabriz, Iran. ⁹Department of Computer Engineering, Faculty of Engineering and Architecture, Nisantasi University, Istanbul, Turkey. ¹⁰Software Engineering Department, Faculty of Engineering and Natural Sciences, Istinye University, Istanbul, Turkey. ¹¹Laboratory of Systems Biology and Bioinformatics (LBB), Institute of Biochemistry and Biophysics, University of Tehran, Tehran, Iran. ✉email: habib_moti@ut.ac.ir; Mokhtarzadehah@tbzmed.ac.ir

small cell lung cancer (SCLC). NSCLC is the most common lung cancer². Histopathological grading has identified about 85% to 90% of lung cancers as NSCLC and 15% to 20% as SCLC³. This cancer includes three different types of Adenocarcinoma, Squamous cell carcinoma, and large cell carcinoma.

Different studies based on computational approaches and network analysis have been undertaken to find biomarker genes for early NSCLC detection. Moreover, scientists have evaluated and discussed the effect of current drugs on this cancer. Based on a co-expression network analysis, Ling Kui et al.⁴ proposed several important genes as biomarkers for NSCLC treatment. Xiujuan Gao et al.⁴ applied the gene expression profile of NSCLC samples and, based on a systems biology approach, reported Estrogen receptors (ERs) as promoters of NSCLC progression. In another study, Mei Zhao et al.⁵ introduced five genes, including *FGF2*, *GOLM1*, *GPC3*, *IL6*, and *SPPI*, which deregulated in NSCLC tissues. They introduced these 5 genes for NSCLC prognosis in patients. A computational approach based on protein–protein interaction (PPI) network analysis was used in a similar study, and Stratifin had an important role in NSCLC⁶ development. Furthermore, Yun-Qiang Zhang et al.⁷ proposed *HIST1H2BH* and *PLK1* as prognostic biomarkers for NSCLC patients.

Drug repositioning (DR) is utilized as a time- and cost-effective method to discover new drugs^{8–12}. Drug repositioning is also referred to as drug repurposing, drug therapeutic, drug recycling, and drug reprofiling^{13,14}. There are usually three kinds of methods for drug repurposing, including experimental biological methods, computational methods, and mixed methods^{10,15,16}. Computational methods can be referred to as molecular docking, network mapping, signature matching, genetic association, and retrospective clinical analysis^{13,17,18}. In the current study, a computational drug repositioning method is applied to identify candidate drugs to treat NSCLC.

Lately, various studies based on the network approach for drug repurposing have been carried out. Network-based strategy is one of the important computational methods in drug repurposing^{19,20}. SAveRUNNER²¹ is a network-based algorithm in this field. This algorithm predicts drug–disease relations based on a similarity measure. This method was provided as an R programming language package²². Xing Li and colleagues²³ proposed a network-based approach to discover lncRNA biomarkers in human lung adenocarcinoma. Furthermore, a computational approach for drug repurposing based on the system biology approach was proposed by Azam Peyvandipour and colleagues²⁴ in 2018. In another study, Wei-Feng Guo et al.²⁵ proposed a network controllability-based algorithm called combinatorial drug identification algorithm (CPGD). Besides, Albert Li and colleagues²⁶ proposed a network-based method, namely LncTx, to repurpose drugs in lung cancer. In a recent study by Zahra and her colleagues²⁷, they proposed a novel network-based method to discover candidate drugs for bladder cancer.

Anisha et al.²⁸ presented an overview of drug repositioning for anti-cancer applications, and they proposed a novel drug repurposing technique to target the MAPK signaling pathway in NSCLC. In a similar study, Muthu Kumar and colleagues²⁹ introduced another drug repurposing method for NSCLC, and they hypothesized that Nebivolol is an excellent candidate for inhibiting MEK in NSCLC patients. In another study, Joelle C. Boulos and colleagues³⁰ repurposed ALK Inhibitor Crizotinib for NSCLC, Acute Leukemia, and Multiple Myeloma Cells. Compared to the mentioned methods, this study applies a novel computational model based on gene co-expression and TF–TG interaction networks. Moreover, two drug–gene interaction networks, including drug–TF and drug–TG, were studied that have not been studied in previous studies.

Gene co-expression network analysis is one of the important network-based approaches in systems biology^{11,31,32}. Different studies based on gene co-expression network analysis were done on different transcriptomic datasets. In this study, a gene co-expression network analysis was applied on the NSCLC transcriptomics dataset to repurpose some potent candidate drugs for NSCLC. Xue-Tao Li³³ and colleagues applied gene co-expression modules analysis in order to predict non-small cell lung cancer survivals. In a similar project, Guanghui Wang et al.³⁴ applied gene co-expression modules analysis on NSCLC metastases.

Weighted gene co-expression network analysis (WGCNA³⁵) is a bioinformatics and systems biology tool that is employed to construct and analyze co-expression networks. This tool is an R programming language package and contains different functions for network construction, visualization, data simulation and gene selection and can be applied for detecting modules (clusters) of highly correlated genes³⁶. In the present study, WGCNA was utilized to reconstruct and analyze the gene co-expression network for NSCLC transcriptomic dataset. Xuting Xu and colleagues³⁷ applied WGCNA to identify hub genes as biomarkers in lung cancer and introduced *CCNB1*, *CCNE2*, *MCM7*, and *PCNA* as hub biomarker genes. In a similar study, Binglin Chen et al.³⁸ applied WGCNA on the NSCLC transcriptomics dataset and identified four hub genes (*AURKB*, *CDC20*, *TPX2*, and *KIF2C*) as NSCLC prognostic biomarkers based on co-expression network analysis. Moreover, WGCNA was utilized to discover prognostic markers in lung cancer by Bo Ling colleague³⁹.

The current study aimed to discover potent candidate drugs for NSCLC treatment by analyzing gene co-expression, TF–TG, and drug–gene interaction networks. To this end, at first, a gene co-expression network was reconstructed based on the WGCNA for the NSCLC transcriptome dataset. Then, two significant gene modules, named *purple* and *magenta*, were discovered from the reconstructed gene co-expression network. Next, a list of transcription factor (TF) genes regulating *purple* and *magenta* modules' genes was gathered from the TRRUST V2.0⁴⁰ online database. Afterward, a TF–gene interaction network was reconstructed for the gathered TFs and their target genes. This network is named the TF–TG network. Simultaneously, Gene Ontology (GO) and pathway enrichment analysis were done using the David bioinformatics Resources 6.8⁴¹ for *purple* and *magenta* modules' genes, and the results were reported. Subsequently, in order to identify the existing drugs targeting TF–TG network genes, the DGIdb V4.0⁴² online database was utilized. After obtaining a list of drugs targeting the TF–TG genes, we reconstructed two drug–gene interaction networks, including drug–TF and drug–TG. Consequently, for each of the drug–TF and Drug–TG networks, nine high-degree drugs (hub drugs) were selected and reported as potent candidate drugs. METHOTREXATE is a hub node in the drug–TG interaction network and regulates 6 genes of the *purple* and *magenta* modules. The highest degree drug node in the drug–TF interaction network is *CISPLATIN*, which regulates 11 TF genes.

In summary, the current study consists of the following three main steps: (1) Gene co-expression network reconstruction, (2) TF-TG interaction network analysis, and (c) Drug-Target interaction network analysis. Compared to the other studies, steps (2) and (3) are novel in our project and have not been applied for drug repurposing for NSCLC before. Moreover, the current study analyses interactions between drugs and both of TFs and non-TF genes (Drug-TF and Drug-TG), which have not been studied before for NSCLC treatment. Figure 1 shows the workflow diagram of the proposed approach.

Result

Module analysis. For 4218 differentially expressed genes between normal and NSCLC, the gene co-expression network was reconstructed for NSCLC transcriptomics data using the WGCNA. Accordingly, 21 gene modules were discovered from this network (Supplementary Fig. C). The *darkorange* module is the smallest module with 47 genes, while the largest module is *blue* with 326 genes. The *grey* module shows genes that are not assigned to any other detected modules. This module is not considered for further analysis.

Comparing the modules between NSCLC and normal groups. Those modules that have changed significantly between NSCLC and normal groups could deregulate some biological processes and cause disease. Therefore, no-preserve modules between NSCLC and normal groups may cause the NSCLC. As described in the method section, the modules with $Z_{summary} < 2$ are considered as no preservation modules for additional analysis. In this regard, the *purple* and *magenta* modules have $Z_{summary} = 0.93$ and $Z_{summary} = 1.3$, respectively and are considered as no preservation modules between NSCLC and normal groups (see Fig. 2). These modules can represent cancer progression from normal to NSCLC stage. Table 1 shows all extracted modules along with their $Z_{summary}$.

Enrichment analysis of the gene modules. In order to study the biological functions of the genes in *purple* and *magenta* modules, functional enrichment analysis was performed using the DAVID⁵ (Database for Annotation Visualization and Integrated Discovery) database. Gene Ontology (GO) enrichment analysis shows that the genes of *purple* and *magenta* modules are enriched in 55 and 72 significant ($p_value < 0.05$) terms, respectively. The results show that the genes in the *purple* module are significantly enriched in some biological processes related to respiration and lung including: *lung epithelial cell differentiation* ($p_value < 0.001$), *lung cell differentiation* ($p_value < 0.001$), *lung epithelium development* ($p_value < 0.004$), *respiratory system development* ($p_value < 0.006$), and *lung development* ($p_value < 0.01$). As well as, the results show that the genes in the *magenta* module are not significantly enriched in biological processes related to respiration and lung. Therefore, the *purple* module genes are closer to NSCLC than the *magenta* module. More details for the GO results are reported in supplementary file S2.

Moreover, to investigate biological pathways related to the purple and magenta modules, the pathway enrichment analysis was done based on the REACTOME⁴⁴ database. The results revealed that the *purple* module is significantly enriched in the regulation of the *insulin secretion* pathway. In addition, the *magenta* module is significantly enriched in five biological pathways, including *Gap junction assembly*, *TP53 Regulates Metabolic Genes*, *Tandem of pore domain in a weak inwardly rectifying K⁺ channels (TWIK)*, *Tight junction interactions*, and *Synthesis of 12-eicosatetraenoic acid derivatives* (see supplementary file S2).

TF-TG regulatory network. In order to identify a list of transcription factor (TF) genes that regulate *magenta* and *purple* modules' genes, the TF-TG regulatory network was reconstructed. Regulatory information of TFs and TGs was retrieved from the TRRUST⁴⁰ online database. After reconstructing the TF-TG regulatory network for *magenta* and *purple* modules, we obtained a network with 178 nodes and 182 regulatory interactions. This network contains 107 TFs and 71 TGs. In this network, *MUC1* with 11 input degrees and *SP1* with 16 output degrees are high TG and TF nodes, respectively. Figure 3 shows the TF-TG regulatory network. A list of TF-TG regulatory interactions is reported in supplementary file S3.

Drug-TG and Drug-TF Interaction networks. The Drug Gene Interaction Database (DGIdb⁴²) was used to detect potential drugs for NSCLC treatment. This database is comprehensive and contains drug-gene interaction information. Using DGIdb, we found 277 candidate drugs that target *purple* and *magenta* modules' genes. These drugs could have a regulatory effect on NSCLC progression. The drug-gene interaction network was reconstructed based on the obtained drugs and the *purple* and *magenta* modules' genes. The Cytoscape⁴³ v.3.8.2 software was used to reconstruct and visualize this network. This network is shown in Fig. 4, and further details are reported in Supplementary file S4. This network shows nine drugs, including Methotrexate, Olanzapine, Haloperidol, Fluorouracil, Nifedipine, Paclitaxel, Verapamil, Dexamethasone, and Docetaxel, are high-degree nodes. These nine drugs, along with target genes, are selected from the network, and then a sub-network is drawn for these drugs and genes (see Fig. 5). In this sub-network, expression levels of genes in NSCLC samples compared to normal samples are shown with blue (Down-Regulation) to red (Up-Regulation) colors. Among these genes, *UGT1A9* has the highest up-regulation, and *ATPIA2* has the highest down-regulation expression level in NSCLC group compared to the normal group. METHOTREXATE is a hub node in this sub-network and regulates 6 genes of the *purple* and *magenta* modules. High-degree drugs in the network regulate more genes and can have important regulatory effects. The details of target genes' expression level in 9 drugs of NSCLC group compared to the normal group are reported in Supplementary file S6.

Moreover, a list of drugs that target those TFs regulating *magenta* and *purple* genes was retrieved from the DGIdb database. A list of TFs with regulatory relationships with *magenta* and *purple* modules' genes is available in supplementary files S3. Supplementary Fig. D shows the Drug-TF interaction network, and the details of this

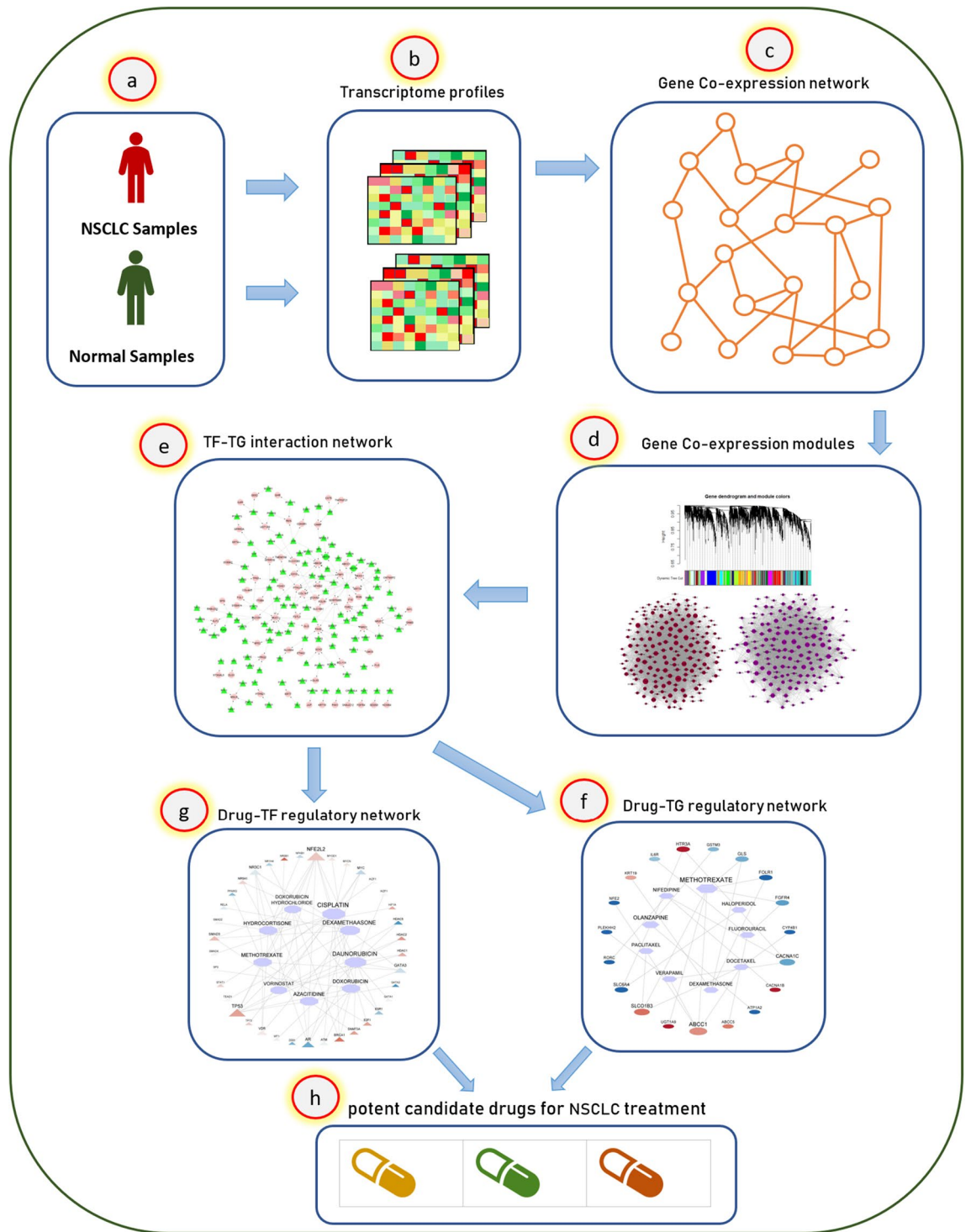


Figure 1. The workflow diagram of the proposed method. This study applies a gene co-expression network and a drug–gene regulatory network analysis to reposition candidate drugs for NSCLC treatment. (a,b) At first, a transcriptome profile for normal and NSCLC samples was downloaded from the GEO database with the accession number GSE21933. (c,d) Then, a gene co-expression network was reconstructed for the differentially expressed genes ($p\text{-value} < 0.01$) of normal and NSCLC groups using the WGCNA package in the R programming environment, and two significant gene modules (*purple* and *magenta*) were extracted from the NSCLC co-expression network. (e) Next, a list of transcription factor genes, which regulate *purple* and *magenta* modules' genes, were obtained from the Trrust V2.0⁴⁰ online database. (f,g) Subsequently, two drug–gene interaction networks, named drug-TG (target gene) and drug-TF (transcription factor gene), were drawn using the DGIdb V4.0⁴² online database. (e) Finally, 18 candidate drugs are proposed for NSCLC treatment.

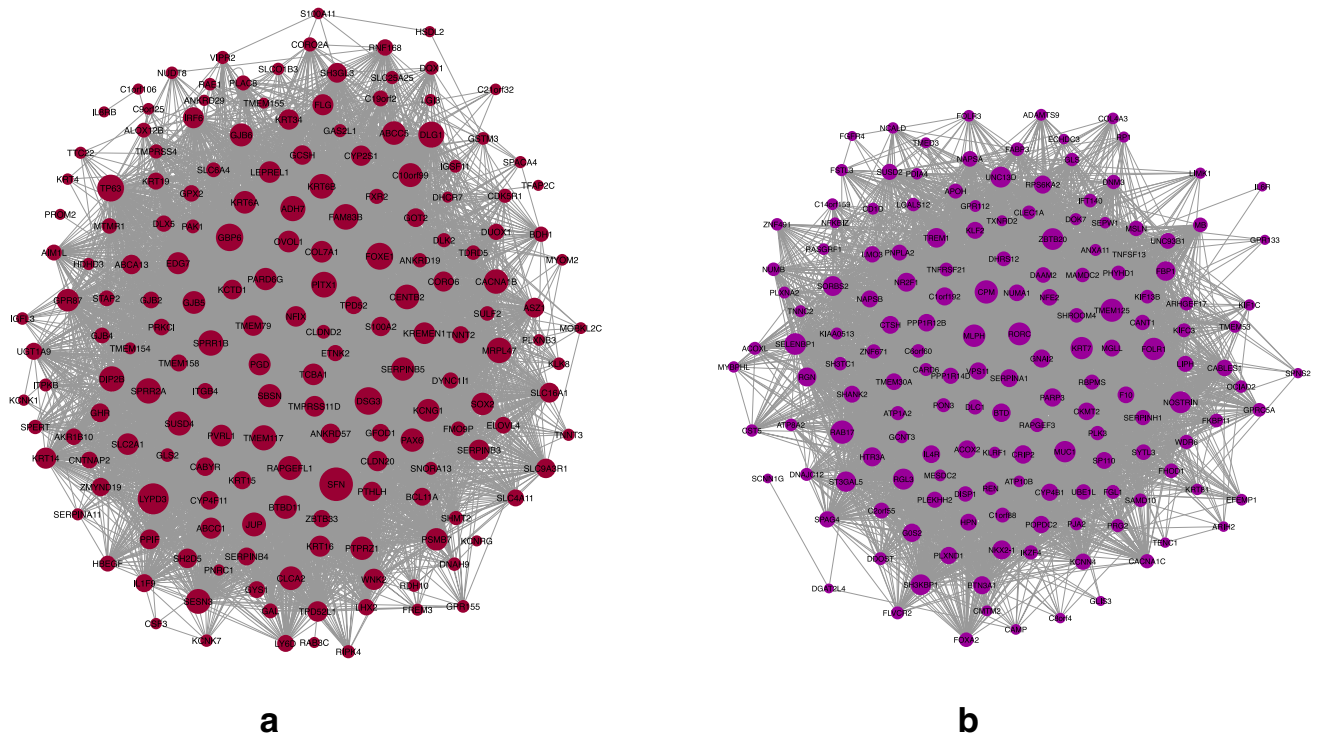


Figure 2. *Magenta (a) and Purple (b) modules.* The circle nodes represent genes (this figure was drawn in the Cytoscape⁴³ v.3.8.2 software).

Module name	Size	Zsummary
Purple	167	0.93
Magenta	183	1.3
Orange	52	2.2
Darkgreen	81	2.7
Red	222	3.5
Grey60	101	4
Midnightblue	112	4.3
Greenyellow	160	4.6
Lightgreen	92	4.6
Cyan	133	5.5
Darkred	84	5.5
Lightcyan	108	5.8
Lightyellow	90	5.8
Darkturquoise	70	6.7
Brown	317	6.9
Blue	326	7.4
Royalblue	87	8.1
Darkorange	47	10
Salmon	140	14
Gold		17
Black	192	27
Grey	42	0.46

Table 1. The Zsummary of NSCLC co-expression modules compared to the normal gene expression data.

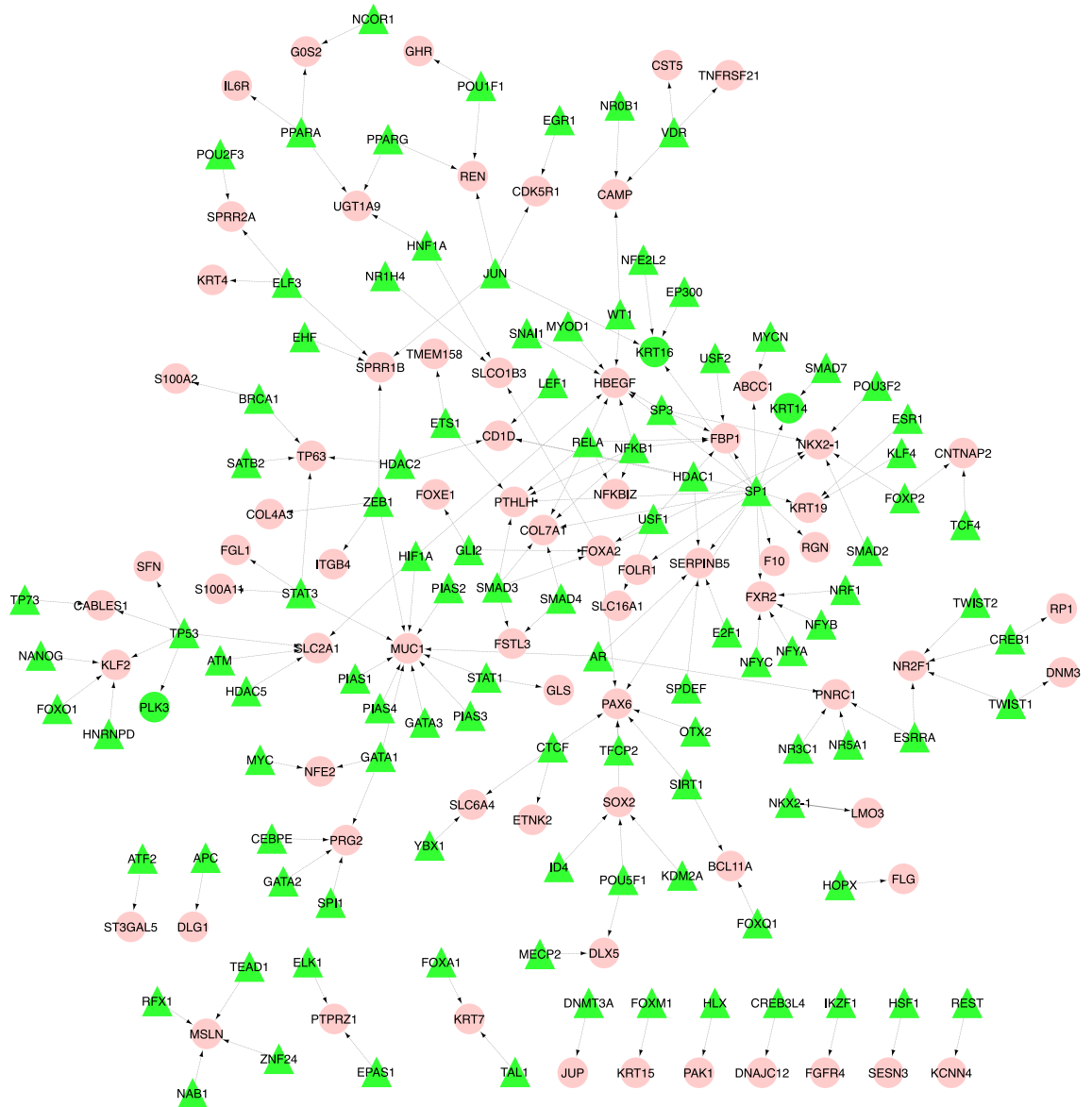


Figure 3. The TF–TG interaction network. This network contains 178 nodes and 182 regulatory interactions. Out of 178 nodes, 107 and 71 nodes are TFs and TGs, respectively. All of the TG nodes are from the *magenta* and *purple* modules. The red circles and green triangles represent TGs and TFs, respectively (this figure was drawn in the Cytoscape⁴³ v.3.8.2 software).

network are reported in Supplementary file S5. This network contains 723 nodes, including 675 drugs and 48 TFs. The highest degree drug node is *Cisplatin* which regulates 11 TF genes, including *NFE2L2*, *TP53*, *ESR1*, *BRCA1*, *ATM*, *MYC*, *E2F1*, *SMAD4*, *MYCN*, *TP73*, and *STAT1*. *Daunorubicin* is the second highest degree drug node that regulates ten TF genes. Among all drugs, those with degree 7 or above along with target TFs were selected from the network, and then a sub-network was drawn for these drugs and TFs. Figure 6 shows this drug–TF sub-network. In this sub-network, the expression level of TF genes in NSCLC samples compared to normal samples is demonstrated with blue (Down-Regulation) to red (Up-Regulation) colors. Furthermore, the TFs' expression level in 9 drugs of the NSCLC group compared to the normal group is reported in Supplementary file S6.

In order to investigate and confirm interactions of the candidate drugs and candidate target genes, the DrugBank⁴⁵ database was used. Information for some candidate drugs and candidate target genes is obtained from this database and reported in Table 2. For some other drugs there were no interaction information.

The literature review of the recent articles shows that most of the proposed candidate drugs have significant effects on NSCLC. *Methotrexate* and *Curcumin* are introduced as novel therapeutic strategies to treat NSCLC⁴⁶. The *Methotrexate* component of MTX–Gd is reported as a chemotherapeutic drug in cancer therapies⁴⁷. Li-Qing Du and colleague noticed that this drug inhibit the expression of RAD51 in cancer cells⁴⁸. Daye Zhang et al. reported that Lenvatinib and Dexamethasone inhibit the invasion and migration of NSCLC⁴⁹. According to Haiyan Ge and colleagues, pemetrexed-induced senescence alleviates in NSCLC by Dexamethasone⁵⁰. In another

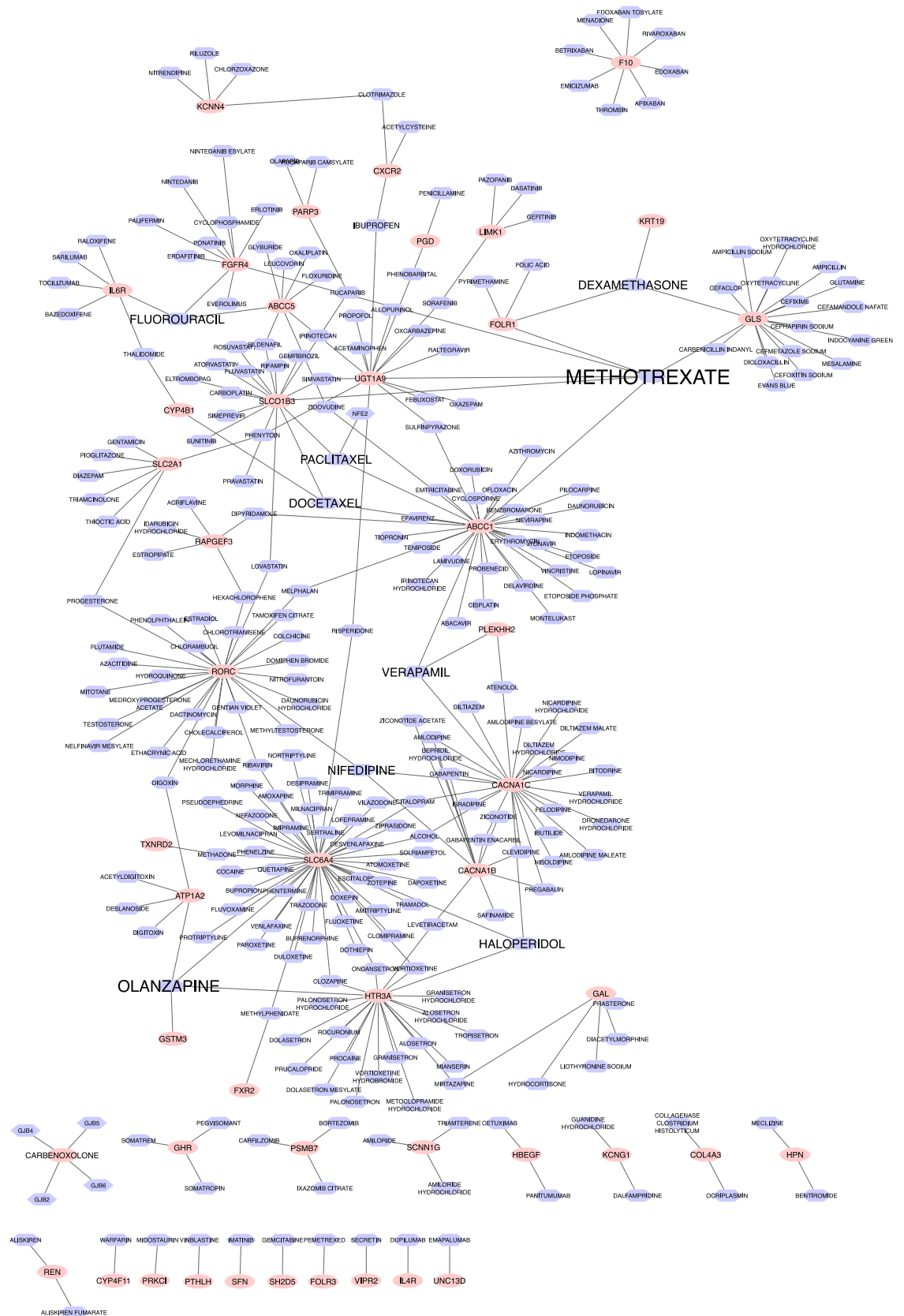


Figure 4. The drug–gene interaction network. Totally, 277 candidate drugs were identified as regulators of the purple and magenta modules of the NSCLC network. The red circle shapes and blue hexagon shapes represent genes and drugs, respectively (this figure was drawn in the Cytoscape⁴³ v.3.8.2 software).

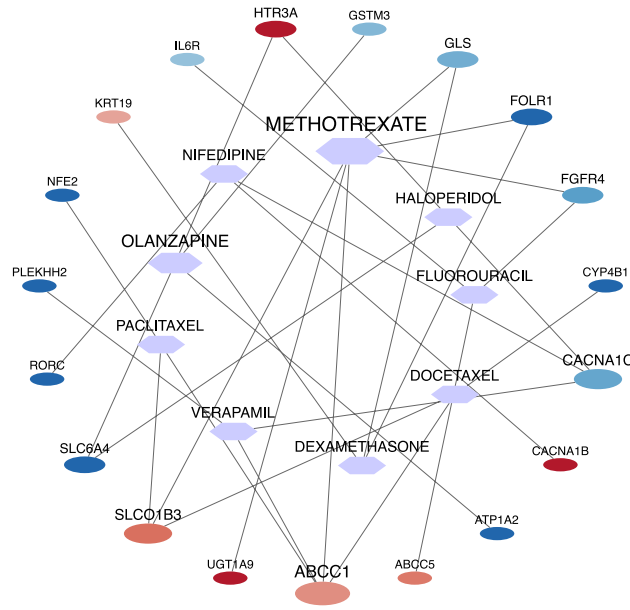


Figure 5. The expression level of hub drugs’ target genes in the NSCLC group compared to the normal group. The circle and hexagon shapes represent genes and drugs, respectively. The size of a node indicates its degree (this figure was drawn in the Cytoscape⁴³ v.3.8.2 software).

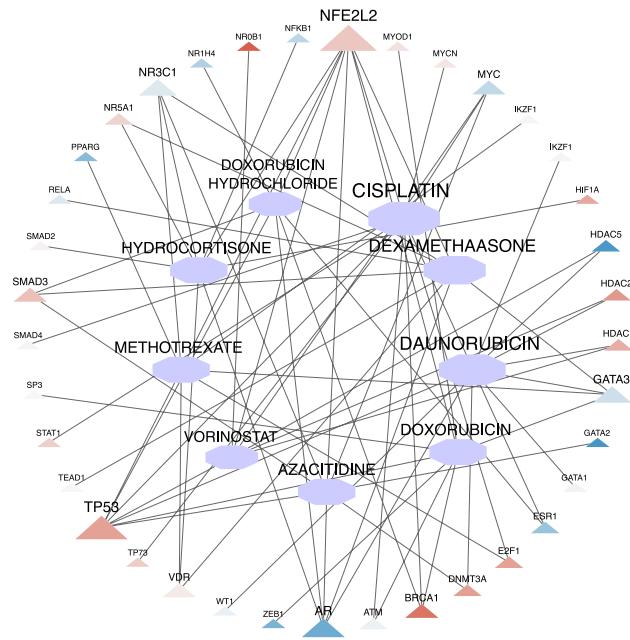


Figure 6. The expression level of hub drugs’ target TFs in NSCLC group compared to the normal group. The triangle and hexagon shapes represent TF genes and drugs, respectively. The size of a node indicates its degree (this figure was drawn in the Cytoscape⁴³ v.3.8.2 software).

study, Tatjana Sarcev and colleagues concluded that Dexamethasone significantly decreases weight and appetite in lung cancer patients⁵¹. Furthermore, Juan P Cata et al. demonstrated that intraoperative Dexamethasone administration to NSCLC patients is not related to its impact on recurrence-free survival (RFS) and overall survival (OS)⁵².

Xin Wang and colleagues revealed that the combination of Ondansetron and Olanzapine has better efficacy in preventing vomiting and chemotherapy-induced nausea in NSCLC patients⁵³. According to Thierry André and colleagues, combining Oxaliplatin, Fluorouracil, and Leucovorin could improve colon cancer treatment⁵⁴. In a similar study, Herbert Hurwitz et al. reported that Bevacizumab and Fluorouracil composition significantly improved the survival among patients with metastatic colorectal cancer⁵⁵. Furthermore, the combination of

Drug name	Type	Target gene
Methotrexate	Transporter	Folate receptor alpha (FOLR1)
Methotrexate	Transporter	Solute carrier organic anion transporter family member 1B3 (SLCO1B3)
Olanzapine	Target	5-Hydroxytryptamine receptor 3A (HTR3A)
Paclitaxel	Transporter	Solute carrier organic anion transporter family member 1B3 (SLCO1B3)
Docetaxel	Transporter	Solute carrier organic anion transporter family member 1B3 (SLCO1B3)
Vorinostat	Target	Histone deacetylase 1 (HDAC1)
Vorinostat	Target	Histone deacetylase 1 (HDAC2)

Table 2. Confirmation of the candidate drugs and candidate target genes thanks to the DrugBank database.

Fluorouracil and Curcumin was studied in cancer treatment by Yumeng Wei and colleagues⁵⁶. Barbora Chovanova and colleagues reported that calcium channel blocker Nifedipine inhibits immune escape and colorectal cancer progression⁵⁷. Moreover, in several studies, it has been proved that Nifedipine can promote breast cancer^{58,59}.

According to Alan Sandler and colleagues, the combination of Paclitaxel, Bevacizumab, and Carboplatin has a significant survival benefit with the risk of increased treatment-related deaths for NSCLC patients⁶⁰. Moreover, Atsuto Mouri and colleagues reported that the combination of Carboplatin and Paclitaxel could be effective and feasible in patients with SCLC, especially those with interstitial lung disease⁶¹. In another study, Dongjie Ma et al. showed that Paclitaxel increases the sensitivity of lung cancer cells to lobaplatin⁶².

Chundi Zhang and colleagues reported that Verapamil might change the expression level of NW23 and EGFR in lung cancer by post-transcriptional and transcriptional levels, respectively⁶³. In addition, S Merry et al. studied the role of Verapamil in overcoming cytotoxic drug resistance in human lung cancer⁶⁴. Zhiyuan Shen and colleagues expressed that circular RNA Foxo3 reduction promotes chemoresistance and prostates cancer progression to Docetaxel⁶⁵. In another study, Hai-Hong Zhou and colleagues recounted that combining Docetaxel and erastin may offer an effective administration for chemo-resistant ovarian cancer patients⁶⁶. Furthermore, Marta Prieto-Vila et al. reported that Quercetin and Docetaxel combination could be a promising therapeutic approach in breast cancer treatment⁶⁷. Juan Valle and colleagues introduced Cisplatin plus Gemcitabine as an effective option for treating advanced biliary cancer⁶⁸. In another study, Deborah K Armstrong and colleagues noted that Cisplatin and Paclitaxel combination improved survival in patients with ovarian cancer⁶⁹. Moreover, Kazumasa Noda et al. reported that Cisplatin plus Irinotecan could effectively treat small-cell lung cancer⁷⁰. According to Ana Catarina Alves and colleagues, Daunorubicin coactions with membranes of cancer cells⁷¹. Furthermore, Yuanyuan Wang and colleagues found that Daunorubicin can be an effective strategy in NSCLC⁷¹ treatment. In a study by Jia Guo and colleagues, the Daunorubicin and Tamoxifen combination was reported as an option to eliminate both cancer stem cells and breast cancer cells⁷². Lilia Antonova and colleagues reported that the expression of the breast cancer susceptibility gene BRCA1 was down-regulated by stress hormone Hydrocortisone in mouse cell line⁷³. Yuan Hong and colleagues reported that Doxorubicin and Curcumin combination could be a method for Lung cancer therapy⁷⁴. In a similar study, Abolfazl Akbarzadeh et al. reported the combination of Doxorubicin β -elemene co-loaded as a way to treat lung cancer⁷⁵. Moreover, Vanesa Gregorc and colleagues showed that the NGR-hTNF plus Doxorubicin could be a way for SCLC⁷⁶ treatment. According to Yang Yang and colleagues' report, Trichostatin and Azacitidine combination decreased tumorigenic of lung cancer cells⁷⁷. Taofeek K Owonikoko and colleagues found that Vorinostat increased Carboplatin and Paclitaxel activity in NSCLC cells⁷⁸. In Sang Eun Park and colleagues' study, Vorinostat and EGFR-TKI combination was evaluated in NSCLC to reverse EGFR-TKI resistance⁷⁹. Furthermore, Chun-Hao Pan and colleagues reported that Vorinostat increased the cisplatin-mediated anticancer effects in SCLC cells⁸⁰. Moreover, Doxorubicin Hydrochloride and Haloperidol were tested on different cancer treatments in humans and other organisms^{81–87}.

Gene set enrichment analysis and candidate drugs validation. In order to validate the proposed drugs for NSCLC treatment, the GSEA was performed based on the Enrichr⁸⁸ database. We considered high-degree drug nodes from the drug-TG sub-network, including *Methotrexate*, *Olanzapine*, *Haloperidol*, *Fluorouracil*, *Nifedipin*, *Paclitaxel*, *Verapamil*, *Dexamethasone*, and *Docetaxel*. In addition, high-degree drug nodes from the drug-TF sub-networks, including *Cisplatin*, *Daunorubicin*, *Dexamethasone*, *Methotrexate*, *Hydrocortisone*, *Doxorubicin*, *Azacitidine*, *Vorinostat*, and *Doxorubicin Hydrochloride*, were considered. Out of these 18 drugs, 2 drugs, including *Dexamethasone* and *Methotrexate*, are common between drug-TG and drug-TF sub-networks. Therefore, 16 drugs are assumed as potent candidate drugs for NSCLC treatment, and the CMAP analysis was performed for these drugs.

The results show that *Methotrexate* and *Paclitaxel* downregulate *GLS2* and *NFE2*, respectively, and *Haloperidol* and *Dexamethasone* up-regulate *HTR3A* and *GLS*, respectively. Moreover, the *Azacitidine* up-regulates the *DNMT 3A* TF gene. Moreover, there was no information regarding other drugs. Romero-Benitez and colleagues studied the impact of paclitaxel on NFE2 in vivo, and they revealed that the expression of NFE2 was up-regulated on day 3⁸⁹. In another study, Anna Schuhmacher et al.⁹⁰ assessed functional and coding variants of the HTR3A subunits in response to haloperidol. Moreover, Takuma Kusabe and colleagues⁹¹ reported that the expression level of GLS is reduced by treatment dexamethasone.

Method

Dataset and preprocessing. In this study, the transcriptomics data with accession number GSE21933 was downloaded from the Gene Expression Omnibus (GEO) database. This data contains 42 male samples, including 21 normal and 21 primary non-small cell lung cancer (NSCLC) samples. The mean and standard deviation of the age for all samples in healthy and NSCLC are about 70 and 7.8, respectively. The annotation file with accession number GPL6254 was used to assign probes to gene IDs.

Hierarchical clustering was done for the normal and NSCLC samples independently to check outlier samples. Results show no outlier samples among the normal and NSCLC samples (see supplementary Fig. A). Therefore, all 42 samples, including normal and NSCLC, are considered for further analysis.

Gene co-expression network and gene modules. First of all, differentially expressed genes (GEGs) were calculated between the normal and NSCLC groups applying the adjusted p-value and Benjamini & Hochberg's method based on the GEO2R tool. Overall, 4218 genes with adjusted p-value less than 0.01 were considered as the initial gene list (see supplementary file S1). This gene list was used in gene co-expression network reconstruction.

Then, the gene co-expression network from NSCLC expression data was reconstructed through the Weighted Gene Co-expression Network Analysis (WGCNA³⁵) package. This package can reconstruct the gene co-expression network in three different ways: "signed", "unsigned", and "signed hybrid". In this project, the type of gene co-expression network is signed hybrid. To adjust the scale-free property of the network, the β (soft thresholding power beta) parameter is applied in this package.

The soft threshold power beta is determined according to the standard scale-free network⁹². This parameter was set to 7 in NSCLC network (see supplementary Fig. B) to gain the scale independency of the network, where the scale-free index R^2 was 0.9. To extract modules for the gene co-expression network, the hierarchical clustering algorithm was applied in WGCNA (see supplementary Fig. C).

Module preservation analysis. To analyze module preservation, the $Z_{summary}$ score was used. The modules with $Z_{summary} < 2$ is considered as no preservation⁹³. The calculation of the $Z_{summary}$ is shown in Eq. (1)⁹⁴. In this equation, $Z_{connectivity}$ and $Z_{density}$ are the connectivity and density of the subnetwork, respectively⁹⁵. The $Z_{summary}$ score in NSCLC network compared to normal data expression is calculated for all extracted modules (see Table 1). It should be noted that the *grey* module shows the genes which are not assigned to other detected modules. Two modules including *purple* and *magenta* (see Fig. 2) have $Z_{summary} < 2$ and considered as no preservation modules. The gene list of these modules is reported in supplementary file S1. These genes could have crucial rules in NSCLC.

$$Z_{summary} = \frac{Z_{connectivity} + Z_{density}}{2} \quad (1)$$

Enrichment analysis. To identify the biological mechanisms of the genes in *purple* and *magenta* modules, we used functional enrichment analysis based on the DAVID^{96,97} (The Database for Annotation, Visualization, and Integrated Discovery) database. Moreover, a pathway enrichment analysis was done for these modules' genes using the Reactome⁹⁸ pathway database.

TF–TG regulatory relationships. In order to obtain regulatory information of Transcription factor (TF) genes and target genes (TG), the TRRUST⁴⁰ V2.0 online database was utilized. TRRUST is a manually curated database containing transcriptional regulatory information for mice and humans. This version of TRRUST contains 8444 TF–TG regulatory information of 800 human TFs. After obtaining TF–TG regulatory relationships, a TF–TG network, which contained TFs regulating *magenta* and *purple* modules' genes, was reconstructed.

Drug–gene interaction network. To identify the candidate drugs that target *purple* and *magenta* genes, the DGIdb⁴² (Drug Gene Interaction Database) was used. This database is connected to 22 other related databases. This database brings back the target genes based on 24 related databases. In the current project, to identify drug–gene interactions information, only experimentally validated interactions were considered.

Gene set enrichment analysis (GSEA). The gene set enrichment analysis (GSEA) was performed as a validation method to test whether the proposed candidate drugs can counteract the gene expression perturbations caused by NSCLC. To this end, the Connectivity Map (CMAP⁹⁹) analysis was performed using the Enrichr⁸⁸ database. To perform the CMAP analysis, the genes of *purple* and *magenta* modules were submitted to the Enrichr⁸⁸ database to retrieve up-regulated or down-regulated genes in the cells treated with different drugs. Two datasets of CMAP-up and CMAP-down, which contained the genes up-regulated or down-regulated by different drugs, were extracted. We queried for our proposed candidate drugs in CMAP-up and CMAP-down datasets. Totally, 16 drugs were proposed as potent candidate drugs for NSCLC treatment, which was evaluated using the Enrichr database.

Guangda Li and colleagues¹⁰⁰ identified some hub genes by combining WGCNA, DEG analysis, and functional enrichment analysis in NSCLC. Moreover, in vitro experiments along with the CMAP database were applied to predict and verify small molecule drugs in NSCLC. These researchers reported cephaeline and Emetine with the potential to overcome resistance using CMAP database. In another study, Ying Zheng et al.¹⁰¹ applied the

CMAP database to predict the anesthetic drugs that regulate the differential expression of RNA binding proteins in cervical squamous cell carcinoma.

They reported 65 differentially expressed RNA binding proteins in cervical squamous cell carcinoma. Moreover, they obtained four anesthetics containing procaine, tetracaine, benzocaine, and pentoxifyverine. Mengnan Zhao and colleagues¹⁰² have done a study in order to identify a prognostic ferroptosis and iron-metabolism signature for esophageal squamous cell carcinoma and they identified 20 potential compounds using CMAP database.

Moreover, Hang Yang et al.¹⁰³ have done multi-omics-based research and they used CMAP for chemotherapy drug analysis and screening for drugs which reduce the expression of high-risk genes. In other study, Zetian Gong and colleague¹⁰⁴, explored several potential small molecule drugs using CMAP based on the mRNAs co-expressed with autophagy-related lncRNAs.

Discussion

This study applied a gene co-expression network analysis to identify potent candidate drugs for NSCLC treatment. To this end, at first, transcriptomics profiles of normal and NSCLC samples were collected, and 4218 genes with a significantly different expression between normal and NSCLC samples were selected for future analysis. Then, a gene co-expression network analysis was reconstructed based on the WGCNA package. Then, two significant gene modules named *purple* and *magenta* were identified. Next, a list of transcription factor genes regulating these two modules' genes was gathered from the TRUST V2.0 online database, and a TF-TG regulatory network was drawn. Subsequently, a list of existing drugs that target TF-TG network genes was collected from the DGIdb V4.0 database, and then two drug-gene interaction networks, including drug-TF and drug-TG, were drawn. In data collection, 675 and 278 drugs were identified for the drug-TF and drug-TG networks, respectively. Consequently, nine high-degree drugs from the drug-TF and drug-TG networks were selected separately and introduced as potent candidate drugs for NSCLC treatment. Eventually, 16 drugs were introduced as potent candidate drugs to treat NSCLC. Out of 16 selected drugs, nine drugs (*Methotrexate*, *Olanzapine*, *Haloperidol*, *Fluorouracil*, *Nifedipine*, *Paclitaxel*, *Verapamil*, *Dexamethasone*, and *Docetaxel*) were selected from the drug-TG network, and nine drugs (*Cisplatin*, *D Daunorubicin*, *Dexamethasone*, *Methotrexate*, *Hydrocortisone*, *Doxorubicin*, *Azacitidine*, *Vorinostat* and *Doxorubicin Hydrochloride*) were selected from the drug-TF sub-network. Out of these 18 hub drugs, *Methotrexate* and *Dexamethasone* are common in drug-TF and drug-TG networks.

In order to evaluate the gene ontology and biological pathways for *purple* and *magenta* modules' genes, the DAVID online tool was used. *Magenta* and *purple* modules were enriched in 72 and 55 Go terms with a $p_value < 0.05$, respectively. The results showed that *purple* and *magenta* modules were more significantly enriched in *phospholipid translocation biological process* with a $p_value \approx 0.0007$ and *skin development biological process* with a $p_value < 1.015e-9$, respectively. Moreover, five significant biological process terms of purple module are related to lung and respiratory. These five significant terms are: lung epithelial cell differentiation ($p_value < 0.001$), lung cell differentiation ($p_value < 0.001$), lung epithelium development ($p_value < 0.004$), respiratory system development ($p_value < 0.006$), and lung development ($p_value < 0.01$). Whereas, none of the significant biological process terms of magenta module are related to lung and respiratory. In conclusion, the purple module genes can be important compared to the magenta module in NSCLC studies.

In addition, a pathway enrichment analysis was done for these two modules based on the REACTOME database. The results show that the purple module was significantly enriched in the "regulation of the insulin secretion" pathway. Three genes of the purple module, including *CACNA1C*, *RAPGEF3*, and *GNAI2*, are involved in the regulation of the insulin secretion pathway. Talip Zengin et al.¹⁰⁵ introduced the *RAPGEF3* for prognostic risk prediction according to overall survival time for lung adenocarcinoma patients. Xiao Wang and colleagues¹⁰⁶ have done genome sequencing analysis for lung adenocarcinoma and introduced *CACNA1C* as a cancer-related gene. Moreover, they reported that this gene was mutated in lung adenocarcinoma tumor tissue. Furthermore, the magenta module was significantly enriched in five biological pathways, including: "Gap junction assembly", "TP53 Regulates Metabolic Genes", "Tandem of pore domain in a weak inwardly rectifying K+ channels (TWIK)", "Tight junction interactions", and "Synthesis of 12-eicosatetraenoic acid derivatives".

The "Gap junction assembly" pathway involves four magenta module genes (*GJB2*, *GJB4*, *GJB5*, *GJB6*). Deng Yun Li et al.¹⁰⁷ and Seon-Sook Han et al.¹⁰⁸ reported that *GJB2* expression is aberrantly higher in Lung adenocarcinoma than in control tissue. In a study that Yi-Pei Lin and colleagues¹⁰⁹ have done, *GJB4* was reported as a novel biomarker for lung cancer. "TP53 Regulates Metabolic Genes" pathway involves five genes of the magenta module containing *GPX2*, *SESN3*, *GLS2*, *SFN*, and *TP63*. In their research, Kui Liu et al.¹¹⁰ revealed that up-regulation of *GPx2* is correlated with worse overall survival for NSCLC patients. Besides, Shuhao Li and colleagues¹¹¹ reported that *SESN3* has high expression in lung cancer patients compared to healthy patients.

Moreover, this gene was reported as an oncogene in esophageal squamous cell carcinoma cells¹¹². Rakibul Islam et al.^{107,113} have done a survival analysis, and their results show a worse overall survival value for *SFN*, and Outcomes show that *SFN* may play a crucial role in the development of NSCLC. "Tandem of pore domain in a weak inwardly rectifying K+ channels (TWIK)" pathway involves two genes of the magenta module, including *KCNK7* and *KCNK1*. Wen Wang and colleagues¹¹⁴ constructed a ceRNA network, and they concluded that *KCNK1* is specific to *LINC00467* in Lung adenocarcinoma. The "Tight junction interactions" pathway involves three genes of the magenta module containing *PRKCI*, *CLDN20*, and *PARD6G*. Yongfeng Wu et al.¹¹⁵ demonstrated that mutation of *PRKCI* and some other genes are identified to be correlated with NSCLC metastasis.

Similarly, Fei Yuan and colleagues¹¹⁶ reported that *PARD6G* is differentially expressed between Lung adenocarcinoma and lung squamous cell cancer. Finally, the last significant pathway for the magenta module is "Synthesis of 12-eicosatetraenoic acid derivatives". This pathway contains two genes of the magenta module containing *GPX2* and *ALOX12B*. Szymon Zmorzyński et al.¹¹⁷ showed that the changes in the activity of the

GPX2 isoform might be associated with other cancers development. In another study, Chao Ma et al.¹¹⁸ reported that ALOX12B could predict lung adenocarcinoma accurately.

Conclusion

In conclusion, we used a gene co-expression network analysis to identify potent candidate drugs for the NSCLC treatment in this study. To this end, at first, a gene co-expression network was reconstructed for the transcriptomics data of the NSCLC patients. Then, two significant gene modules, namely *magenta* and *purple*, were discovered from the constructed co-expression network. After that, a *TF-TG* regulatory network was drawn for *magenta* and *purple* modules' genes and the TFs targeting these modules' genes. Next, two drug-gene interaction networks, namely *drug-TG* and *drug-TF*, were constructed. Subsequently, from each *drug-TG* and *drug-TF* network, nine high-degree drugs were selected and reported as potent candidates for NSCLC treatment. Consequently, 16 drugs, including *Methotrexate*, *Olanzapine*, *Haloperidol*, *Fluorouracil*, *Nifedipine*, *Paclitaxel*, *Verapamil*, *Dexamethasone*, *Docetaxel*, *Cisplatin*, *Daunorubicin*, *Hydrocortisone*, *Doxorubicin*, *Azacitidine*, *Vorinostat*, and *Doxorubicin Hydrochloride*, were introduced as potent candidate drugs to treat NSCLC. Moreover, gene ontology and pathway enrichment analyses were run for the *magenta* and *purple* modules.

Data availability

The corresponding author can provide the datasets utilized in this study on a reasonable request. The raw dataset is available on Information Gene expression Omnibus (GEO) with GSE21933 accession number (<https://www.ncbi.nlm.nih.gov/geo/query/acc.cgi?acc=GSE21933>).

Received: 22 March 2022; Accepted: 16 May 2022

Published online: 08 June 2022

References

- Nasim, F., Sabath, B. F. & Eapen, G. A. Lung cancer. *Med. Clin. N. Am.* **103**, 463–473. <https://doi.org/10.1016/j.mcna.2018.12.006> (2019).
- Chen, Z., Fillmore, C. M., Hammerman, P. S., Kim, C. F. & Wong, K.-K. Non-small-cell lung cancers: A heterogeneous set of diseases. *Nat. Rev. Cancer* **14**, 535–546 (2014).
- Langhammer, S. Rationale for the design of an oncology trial using a generic targeted therapy multi-drug regimen for NSCLC patients without treatment options. *Oncol. Rep.* **30**, 1535–1541 (2013).
- Gao, X. et al. Estrogen receptors promote NSCLC progression by modulating the membrane receptor signaling network: A systems biology perspective. *J. Transl. Med.* **17**, 1–15 (2019).
- Zhao, M., Li, X. & Chen, X. GOLM1 predicts poor prognosis of patients with NSCLC and is associated with the proliferation and chemo-sensitivity of cisplatin in NSCLC cells: Bioinformatics analysis and laboratory validation. *J. Bioenerg. Biomembr.* **53**, 177–189 (2021).
- Islam, R. et al. Identification of molecular biomarkers and pathways of NSCLC: Insights from a systems biomedicine perspective. *J. Genet. Eng. Biotechnol.* **19**, 1–9 (2021).
- Zhang, Y.-Q. et al. Evaluation of the roles and regulatory mechanisms of PD-1 target molecules in NSCLC progression. *Ann. Transl. Med.* **9**, 14 (2021).
- Begley, C. G. et al. Drug repurposing: Misconceptions, challenges, and opportunities for academic researchers. *Sci. Transl. Med.* **13**, eabd5524 (2021).
- Adhami, M., Sadeghi, B., Rezapour, A., Haghdoost, A. A. & MotieGhader, H. Repurposing novel therapeutic candidate drugs for coronavirus disease-19 based on protein-protein interaction network analysis. *BMC Biotechnol.* **21**, 1–11 (2021).
- MotieGhader, H., Safavi, E., Rezapour, A. & Amoodizaj, F. F. Drug repurposing for coronavirus (SARS-CoV-2) based on gene co-expression network analysis. *Sci. Rep.* **11**, 1–15 (2021).
- Soleimani Zakeri, N. S., Pashazadeh, S. & MotieGhader, H. Drug repurposing for Alzheimer's disease based on protein-protein interaction network. *Biomed. Res. Int.* **2021**, 1280237. <https://doi.org/10.1155/2021/1280237> (2021).
- Masoudi-Sobhanzadeh, Y., Omidi, Y., Amanlou, M. & Masoudi-Nejad, A. DrugR+: A comprehensive relational database for drug repurposing, combination therapy, and replacement therapy. *Comput. Biol. Med.* **109**, 254–262 (2019).
- Pushpakom, S. et al. Drug repurposing: Progress, challenges and recommendations. *Nat. Rev. Drug Discov.* **18**, 41–58 (2019).
- Hooshmand, S. A. et al. A multimodal deep learning-based drug repurposing approach for treatment of COVID-19. *Mol. Divers.* **25**, 1717–1730 (2021).
- Xue, H., Li, J., Xie, H. & Wang, Y. Review of drug repositioning approaches and resources. *Int. J. Biol. Sci.* **14**, 1232 (2018).
- Soleimani Zakeri, N. S., Pashazadeh, S. & MotieGhader, H. Drug repurposing for Alzheimer's disease based on protein-protein interaction network. *BioMed Res. Int.* **2021**, 14 (2021).
- Ghasemi, M., Seidkhani, H., Tamimi, F., Rahgozar, M. & Masoudi-Nejad, A. Centrality measures in biological networks. *Curr. Bioinform.* **9**, 426–441 (2014).
- Moti Ghader, H., KeyKhosravi, D. & HosseinAliPour, A. *Asian Conference on Intelligent Information and Database Systems*. 247–257 (Springer, 2021).
- Conte, F. et al. A paradigm shift in medicine: A comprehensive review of network-based approaches. *Biochim. Biophys. BBA Acta Gene Regulat. Mech.* **1863**, 194416 (2020).
- Kouhsar, M., AzimzadehJamalkandi, S., Moeini, A. & Masoudi-Nejad, A. Detection of novel biomarkers for early detection of non-muscle-invasive bladder cancer using competing endogenous RNA network analysis. *Sci. Rep.* **9**, 1–15 (2019).
- Fiscon, G., Conte, F., Farina, L. & Paci, P. SAveRUNNER: A network-based algorithm for drug repurposing and its application to COVID-19. *PLoS Comput. Biol.* **17**, e1008686 (2021).
- Fiscon, G. & Paci, P. SAveRUNNER: An R-based tool for drug repurposing. *BMC Bioinform.* **22**, 1–10 (2021).
- Li, X., Li, B., Ran, P. & Wang, L. Identification of ceRNA network based on a RNA-seq shows prognostic lncRNA biomarkers in human lung adenocarcinoma. *Oncol. Lett.* **16**, 5697–5708 (2018).
- Peyvandipour, A., Saberian, N., Shafi, A., Donato, M. & Draghici, S. A novel computational approach for drug repurposing using systems biology. *Bioinformatics* **34**, 2817–2825 (2018).
- Guo, W.-F. et al. Network controllability-based algorithm to target personalized driver genes for discovering combinatorial drugs of individual patients. *Nucleic Acids Res.* **49**, e37–e37 (2021).
- Li, A., Huang, H.-T., Huang, H.-C. & Juan, H.-F. LncTx: A network-based method to repurpose drugs acting on the survival-related lncRNAs in lung cancer. *Comput. Struct. Biotechnol. J.* **19**, 3990–4002 (2021).

27. Abedi, Z., Motieghader, H., Hosseini, S. S., Sheikh BeigGoharrizi, M. A. & Masoudi-Nejad, A. mRNA–miRNA bipartite networks reconstruction in different tissues of bladder cancer based on gene co-expression network analysis. *Sci. Rep.* **12**, 1–17 (2022).
28. Jain, A. S. *et al.* Everything old is new again: Drug repurposing approach for non-small cell lung cancer targeting MAPK signaling pathway. *Front. Oncol.* **11**, 741326. <https://doi.org/10.3389/fonc.2021.741326> (2021).
29. Thirunavukkarasu, M. K. & Karuppasamy, R. Drug repurposing combined with MM/PBSA based validation strategies towards MEK inhibitors screening. *J. Biomol. Struct. Dyn.* <https://doi.org/10.1080/07391102.2021.1970629> (2021).
30. Boulos, J. C. *et al.* Repurposing of the ALK inhibitor crizotinib for acute leukemia and multiple myeloma cells. *Pharmaceuticals* **14**, 1126 (2021).
31. Motieghader, H., Kouhsar, M., Najafi, A., Sadeghi, B. & Masoudi-Nejad, A. mRNA–miRNA bipartite network reconstruction to predict prognostic module biomarkers in colorectal cancer stage differentiation. *Mol. BioSyst.* **13**, 2168–2180 (2017).
32. Ahmadi, H. *et al.* HomoTarget: A new algorithm for prediction of microRNA targets in *Homo sapiens*. *Genomics* **101**, 94–100 (2013).
33. Li, X.-T. *et al.* Gene co-expression modules integrated with immunoscore predicts survival of non-small cell lung cancer. *Cancer Treat. Res. Commun.* **26**, 100297 (2021).
34. Wang, G. *et al.* Study of the co-expression gene modules of non-small cell lung cancer metastases. *Cancer Biomark.* **30**, 321–329 (2021).
35. Langfelder, P. & Horvath, S. WGCNA: An R package for weighted correlation network analysis. *BMC Bioinform.* **9**, 1–13 (2008).
36. Langfelder, P. & Horvath, S. WGCNA: An R package for weighted correlation network analysis. *BMC Bioinform.* **9**, 559. <https://doi.org/10.1186/1471-2105-9-559> (2008).
37. Ren, W. *et al.* RYR2 mutation in non-small cell lung cancer prolongs survival via down-regulation of DKK1 and up-regulation of GS1-115G20. 1: A weighted gene Co-expression network analysis and risk prognostic models. *IET Syst. Biol.* **16**, 43 (2021).
38. Chen, B., Xie, X., Lan, F. & Liu, W. Identification of prognostic markers by weighted gene co-expression network analysis in non-small cell lung cancer. *Bioengineered* **12**, 4924–4935 (2021).
39. Ling, B. *et al.* Identification of prognostic markers of lung cancer through bioinformatics analysis and in vitro experiments. *Int. J. Oncol.* **56**, 193–205 (2020).
40. Han, H. *et al.* TRRUST v2: An expanded reference database of human and mouse transcriptional regulatory interactions. *Nucleic Acids Res.* **46**, D380–D386 (2018).
41. Huang, D. W., Sherman, B. T. & Lempicki, R. A. Systematic and integrative analysis of large gene lists using DAVID bioinformatics resources. *Nat. Protoc.* **4**, 44–57 (2009).
42. Freshour, S. L. *et al.* Integration of the drug–gene interaction database (DGIdb 4.0) with open crowdsourcing efforts. *Nucleic Acids Res.* **49**, D1144–D1151 (2021).
43. Shannon, P. *et al.* Cytoscape: A software environment for integrated models of biomolecular interaction networks. *Genome Res.* **13**, 2498–2504 (2003).
44. Jassal, B. *et al.* The reactome pathway knowledgebase. *Nucleic Acids Res.* **48**, D498–D503 (2020).
45. Wishart, D. S. *et al.* DrugBank: A comprehensive resource for in silico drug discovery and exploration. *Nucleic Acids Res.* **34**, D668–D672 (2006).
46. Rudnik, L. A. C. *et al.* Co-loaded curcumin and methotrexate nanocapsules enhance cytotoxicity against non-small-cell lung cancer cells. *Molecules* **25**, 1913 (2020).
47. Xu, D. *et al.* Evaluation of methotrexate-conjugated gadolinium (III) for cancer diagnosis and treatment. *Drug Des. Dev. Ther.* **12**, 3301 (2018).
48. Du, L.-Q. *et al.* Methotrexate-mediated inhibition of RAD51 expression and homologous recombination in cancer cells. *J. Cancer Res. Clin. Oncol.* **138**, 811–818 (2012).
49. Zhang, D., Zhang, Y., Cai, Z., Tu, Y. & Hu, Z. Dexamethasone and lenvatinib inhibit migration and invasion of non-small cell lung cancer by regulating EKR/AKT and VEGF signal pathways. *Exp. Ther. Med.* **19**, 762–770 (2020).
50. Ge, H. *et al.* Dexamethasone alleviates pemetrexed-induced senescence in non-small-cell lung cancer. *Food Chem. Toxicol.* **119**, 86–97 (2018).
51. Šarčev, T., Sečen, N., Sabo, A. & Považan, D. Influence of dexamethasone on appetite and body weight in lung cancer patients. *Med. Pregl.* **61**, 571–575 (2008).
52. Cata, J. P. *et al.* Lack of association between dexamethasone and long-term survival after non-small cell lung cancer surgery. *J. Cardiothorac. Vasc. Anesth.* **30**, 930–935 (2016).
53. Wang, X., Wang, L., Wang, H. & Zhang, H. Effectiveness of olanzapine combined with ondansetron in prevention of chemotherapy-induced nausea and vomiting of non-small cell lung cancer. *Cell Biochem. Biophys.* **72**, 471–473 (2015).
54. André, T. *et al.* Oxaliplatin, fluorouracil, and leucovorin as adjuvant treatment for colon cancer. *N. Engl. J. Med.* **350**, 2343–2351 (2004).
55. Hurwitz, H. *et al.* Bevacizumab plus irinotecan, fluorouracil, and leucovorin for metastatic colorectal cancer. *N. Engl. J. Med.* **350**, 2335–2342 (2004).
56. Wei, Y., Yang, P., Cao, S. & Zhao, L. The combination of curcumin and 5-fluorouracil in cancer therapy. *Arch. Pharmacol. Res.* **41**, 1–13 (2018).
57. Chovancova, B. *et al.* Calcium signaling affects migration and proliferation differently in individual cancer cells due to nifedipine treatment. *Biochem. Pharmacol.* **171**, 113695 (2020).
58. Zhao, T., Guo, D., Gu, Y. & Ling, Y. Nifedipine stimulates proliferation and migration of different breast cancer cells by distinct pathways. *Mol. Med. Rep.* **16**, 2259–2263 (2017).
59. Guo, D.-Q., Zhang, H., Tan, S.-J. & Gu, Y.-C. Nifedipine promotes the proliferation and migration of breast cancer cells. *PLoS ONE* **9**, e113649 (2014).
60. Sandler, A. *et al.* Paclitaxel–carboplatin alone or with bevacizumab for non–small-cell lung cancer. *N. Engl. J. Med.* **355**, 2542–2550 (2006).
61. Mouri, A. *et al.* Combination therapy with carboplatin and paclitaxel for small cell lung cancer. *Respir. Investig.* **57**, 34–39 (2019).
62. Ma, D. *et al.* Paclitaxel increases the sensitivity of lung cancer cells to lobaplatin via PI3K/Akt pathway. *Oncol. Lett.* **15**, 6211 (2018).
63. Zhang, C. *et al.* Effect of verapamil on the expression of EGFR and NM23 in A549 human lung cancer cells. *Anticancer Res.* **29**, 27–32 (2009).
64. Merry, S., Courtney, E., Fetherston, C., Kaye, S. & Freshney, R. Circumvention of drug resistance in human non-small cell lung cancer in vitro by verapamil. *Br. J. Cancer* **56**, 401–405 (1987).
65. Shen, Z., Zhou, L., Zhang, C. & Xu, J. Reduction of circular RNA Foxo3 promotes prostate cancer progression and chemoresistance to docetaxel. *Cancer Lett.* **468**, 88–101 (2020).
66. Zhou, H.-H. *et al.* Erastin reverses ABCB1-mediated docetaxel resistance in ovarian cancer. *Front. Oncol.* **9**, 1398 (2019).
67. Prieto-Vila, M. *et al.* Quercetin inhibits Lef1 and resensitizes docetaxel-resistant breast cancer cells. *Molecules* **25**, 2576 (2020).
68. Lin, J. *et al.* (American Society of Clinical Oncology, 2020).
69. Armstrong, D. K. *et al.* Intraperitoneal cisplatin and paclitaxel in ovarian cancer. *N. Engl. J. Med.* **354**, 34–43 (2006).
70. Noda, K. *et al.* Irinotecan plus cisplatin compared with etoposide plus cisplatin for extensive small-cell lung cancer. *N. Engl. J. Med.* **346**, 85–91 (2002).

71. Alves, A. C. *et al.* The daunorubicin interplay with mimetic model membranes of cancer cells: A biophysical interpretation. *Biochim. Biophys. Acta Biomembr.* **1859**, 941–948 (2017).
72. Guo, J. & Lu, W.-L. Effects of stealth liposomal daunorubicin plus tamoxifen on the breast cancer and cancer stem cells. *J. Pharm. Pharm. Sci.* **13**, 136–151 (2010).
73. Antonova, L. & Mueller, C. R. Hydrocortisone down-regulates the tumor suppressor gene BRCA1 in mammary cells: A possible molecular link between stress and breast cancer. *Genes Chromosom. Cancer* **47**, 341–352 (2008).
74. Hong, Y. *et al.* Lung cancer therapy using doxorubicin and curcumin combination: Targeted prodrug based, pH sensitive nano-medicine. *Biomed. Pharmacother.* **112**, 108614 (2019).
75. Cao, C., Wang, Q. & Liu, Y. Lung cancer combination therapy: Doxorubicin and β -elemene co-loaded, pH-sensitive nanostructured lipid carriers. *Drug Des. Dev. Ther.* **13**, 1087 (2019).
76. Gregorc, V. *et al.* NGR-hTNF and doxorubicin as second-line treatment of patients with small cell lung cancer. *Oncologist* **23**, 1133 (2018).
77. Yang, Y., Yin, W., Wu, F. & Fan, J. Combination of azacitidine and trichostatin A decreased the tumorigenic potential of lung cancer cells. *Onco. Targets. Ther.* **10**, 2993 (2017).
78. Owonikoko, T. K. *et al.* Vorinostat increases carboplatin and paclitaxel activity in non-small cell lung cancer cells. *Int. J. Cancer* **126**, 743–755 (2010).
79. Park, S. E. *et al.* Vorinostat enhances gefitinib-induced cell death through reactive oxygen species-dependent cleavage of HSP90 and its clients in non-small cell lung cancer with the EGFR mutation. *Oncol. Rep.* **41**, 525–533 (2019).
80. Pan, C.-H. *et al.* Vorinostat enhances the cisplatin-mediated anticancer effects in small cell lung cancer cells. *BMC Cancer* **16**, 1–11 (2016).
81. Yaşayan, G., Mega Tiber, P., Orun, O. & Alarçın, E. Doxorubicin hydrochloride loaded nanotextured films as a novel drug delivery platform for ovarian cancer treatment. *Pharm. Dev. Technol.* **25**, 1289–1301. <https://doi.org/10.1080/10837450.2020.1823992> (2020).
82. Xiao, B. *et al.* Doxorubicin hydrochloride enhanced antitumour effect of CEA-regulated oncolytic virotherapy in live cancer cells and a mouse model. *J. Cell Mol. Med.* **24**, 13431–13439. <https://doi.org/10.1111/jcmm.15966> (2020).
83. Di Francesco, M. *et al.* Doxorubicin hydrochloride-loaded nonionic surfactant vesicles to treat metastatic and non-metastatic breast cancer. *ACS Omega* **6**, 2973–2989. <https://doi.org/10.1021/acsomega.0c05350> (2021).
84. Friedman, G. D. *et al.* Haloperidol and prostate cancer prevention: More epidemiologic research needed. *Perm J.* <https://doi.org/10.7812/tpp/18.313> (2020).
85. Hui, D. *et al.* Effect of lorazepam with haloperidol vs haloperidol alone on agitated delirium in patients with advanced cancer receiving palliative care: A randomized clinical trial. *JAMA* **318**, 1047–1056. <https://doi.org/10.1001/jama.2017.11468> (2017).
86. Radha Krishna, L. K., Poulouse, V. J. & Goh, C. The use of midazolam and haloperidol in cancer patients at the end of life. *Singap. Med. J.* **53**, 62–66 (2012).
87. Hardy, J. R. *et al.* Methotrimeprazine versus haloperidol in palliative care patients with cancer-related nausea: A randomised, double-blind controlled trial. *BMJ Open* **9**, e029942. <https://doi.org/10.1136/bmjopen-2019-029942> (2019).
88. Chen, E. Y. *et al.* Enrichr: Interactive and collaborative HTML5 gene list enrichment analysis tool. *BMC Bioinform.* **14**, 1–14 (2013).
89. Romero-Benitez, M. M. *et al.* In vivo erythroid recovery following paclitaxel injury: Correlation between GATA-1, c-MYB, NF-E2, Epo receptor expressions, and apoptosis. *Toxicol. Appl. Pharmacol.* **194**, 230–238. <https://doi.org/10.1016/j.taap.2003.09.009> (2004).
90. Schuhmacher, A. *et al.* Influence of 5-HT₃ receptor subunit genes HTR3A, HTR3B, HTR3C, HTR3D and HTR3E on treatment response to antipsychotics in schizophrenia. *Pharmacogenet. Genomics* **19**, 843–851 (2009).
91. Kusabe, T. *et al.* The inhibitory effect of disease-modifying anti-rheumatic drugs and steroids on gliostatin/platelet-derived endothelial cell growth factor production in human fibroblast-like synoviocytes. *Rheumatol. Int.* **25**, 625–630. <https://doi.org/10.1007/s00296-005-0624-8> (2005).
92. Shi, G., Shen, Z., Liu, Y. & Yin, W. Identifying biomarkers to predict the progression and prognosis of breast cancer by weighted gene co-expression network analysis. *Front. Genet.* **11**, 597888–597888. <https://doi.org/10.3389/fgene.2020.597888> (2020).
93. Langfelder, P., Luo, R., Oldham, M. C. & Horvath, S. Is my network module preserved and reproducible?. *PLoS Comput. Biol.* **7**, e1001057 (2011).
94. Riquelme Medina, I. & Lubovac-Pilav, Z. Gene co-expression network analysis for identifying modules and functionally enriched pathways in type 1 diabetes. *PLoS ONE* **11**, e0156006 (2016).
95. Pavlopoulos, G. A. *et al.* Using graph theory to analyze biological networks. *BioData Mining* **4**, 1–27 (2011).
96. Sherman, B. T. & Lempicki, R. A. Systematic and integrative analysis of large gene lists using DAVID bioinformatics resources. *Nat. Protoc.* **4**, 44 (2009).
97. Huang, D. W., Sherman, B. T. & Lempicki, R. A. Bioinformatics enrichment tools: paths toward the comprehensive functional analysis of large gene lists. *Nucleic Acids Res.* **37**, 1–13 (2009).
98. Fabregat, A. *et al.* The reactome pathway knowledgebase. *Nucleic Acids Res.* **46**, D649–D655 (2018).
99. Lamb, J. *et al.* The Connectivity Map: Using gene-expression signatures to connect small molecules, genes, and disease. *Science* **313**, 1929–1935 (2006).
100. Li, G. *et al.* Identification of hub genes and small molecule drugs associated with acquired resistance to Gefitinib in non-small cell lung cancer. *J. Cancer* **12**, 5286–5295. <https://doi.org/10.7150/jca.56506> (2021).
101. Zheng, Y., Meng, X. W. & Yang, J. P. Exploring potential regulatory anesthetic drugs based on RNA binding protein and constructing CESC prognosis model: A study based on TCGA database. *Front. Surg.* **9**, 823566. <https://doi.org/10.3389/fsurg.2022.823566> (2022).
102. Zhao, M. *et al.* Identification and analysis of a prognostic ferroptosis and iron-metabolism signature for esophageal squamous cell carcinoma. *J. Cancer* **13**, 1611–1622. <https://doi.org/10.7150/jca.68568> (2022).
103. Yang, H. & Jiang, Q. A multi-omics-based investigation of the immunological and prognostic impact of necroptosis-related genes in patients with hepatocellular carcinoma. *J. Clin. Lab Anal.* **36**, e24346. <https://doi.org/10.1002/jcla.24346> (2022).
104. Gong, Z., Li, Q., Li, J., Xie, J. & Wang, W. A novel signature based on autophagy-related lncRNA for prognostic prediction and candidate drugs for lung adenocarcinoma. *Transl. Cancer Res.* **11**, 14–28. <https://doi.org/10.21037/tcr-21-1554> (2022).
105. Zengin, T. & Önal-Süzek, T. Analysis of genomic and transcriptomic variations as prognostic signature for lung adenocarcinoma. *BMC Bioinform.* **21**, 368. <https://doi.org/10.1186/s12859-020-03691-3> (2020).
106. Wang, X. *et al.* Whole genome sequencing analysis of lung adenocarcinoma in Xuanwei, China. *Thorac. Cancer* **8**, 88–96. <https://doi.org/10.1111/1759-7714.12411> (2017).
107. Li, D. Y., Yue, L. X., Wang, S. G. & Wang, T. X. Quercitrin restrains the growth and invasion of lung adenocarcinoma cells by regulating gap junction protein beta 2. *Bioengineered* **13**, 6126–6135. <https://doi.org/10.1080/21655979.2022.2037372> (2022).
108. Han, S. S. *et al.* RNA sequencing identifies novel markers of non-small cell lung cancer. *Lung Cancer* **84**, 229–235. <https://doi.org/10.1016/j.lungcan.2014.03.018> (2014).
109. Lin, Y. P., Wu, J. I., Tseng, C. W., Chen, H. J. & Wang, L. H. Gjb4 serves as a novel biomarker for lung cancer and promotes metastasis and chemoresistance via Src activation. *Oncogene* **38**, 822–837. <https://doi.org/10.1038/s41388-018-0471-1> (2019).

110. Liu, K., Jin, M., Xiao, L., Liu, H. & Wei, S. Distinct prognostic values of mRNA expression of glutathione peroxidases in non-small cell lung cancer. *Cancer Manag. Res.* **10**, 2997–3005. <https://doi.org/10.2147/cmar.S163432> (2018).
111. Li, S., Jiang, L., Tang, J., Gao, N. & Guo, F. Kernel fusion method for detecting cancer subtypes via selecting relevant expression data. *Front. Genet.* **11**, 979. <https://doi.org/10.3389/fgene.2020.00979> (2020).
112. Li, Z. W. *et al.* Small nucleolar RNA host gene 22 (SNHG22) promotes the progression of esophageal squamous cell carcinoma by miR-429/SES3 axis. *Ann. Transl. Med.* **8**, 1007. <https://doi.org/10.21037/atm-20-5332> (2020).
113. Islam, R. *et al.* Identification of molecular biomarkers and pathways of NSCLC: Insights from a systems biomedicine perspective. *J. Genet. Eng. Biotechnol.* **19**, 43. <https://doi.org/10.1186/s43141-021-00134-1> (2021).
114. Wang, W., Bo, H., Liang, Y. & Li, G. LINC00467 Is Upregulated by DNA Copy Number Amplification and Hypomethylation and Shows ceRNA Potential in Lung Adenocarcinoma. *Front. Endocrinol. (Lausanne)* **12**, 802463. <https://doi.org/10.3389/fendo.2021.802463> (2021).
115. Wu, Y. *et al.* Driver and novel genes correlated with metastasis of non-small cell lung cancer: A comprehensive analysis. *Pathol Res Pract* **224**, 153551. <https://doi.org/10.1016/j.prp.2021.153551> (2021).
116. Yuan, F., Lu, L. & Zou, Q. Analysis of gene expression profiles of lung cancer subtypes with machine learning algorithms. *Biochim. Biophys. Acta Mol. Basis Dis.* **1866**, 165822. <https://doi.org/10.1016/j.bbadis.2020.165822> (2020).
117. Zmorzyński, S., Świderska-Kolacz, G., Koczkodaj, D. & Filip, A. A. Significance of polymorphisms and expression of enzyme-encoding genes related to glutathione in hematopoietic cancers and solid tumors. *Biomed. Res. Int.* **2015**, 853573. <https://doi.org/10.1155/2015/853573> (2015).
118. Ma, C., Li, F. & Luo, H. Prognostic and immune implications of a novel ferroptosis-related ten-gene signature in lung adenocarcinoma. *Ann. Transl. Med.* **9**, 1058. <https://doi.org/10.21037/atm-20-7936> (2021).

Author contributions

H.M.G. wrote the main manuscript. P.T.N. and H.M.G. performed the analyses. H.M.G., E.K.H. M.M. and A.M.N. reconstructed and analyzed the networks. M.D.A.P., H.M.G., A.M.N., B.B., A.M., and M.H. interpreted the results and wrote the manuscript. H.L., S.M.J., S.N., F.K. and M.M. analyzed the results. All authors reviewed the manuscript.

Competing interests

The authors declare no competing interests.

Additional information

Supplementary Information The online version contains supplementary material available at <https://doi.org/10.1038/s41598-022-13719-8>.

Correspondence and requests for materials should be addressed to H.M. or A.M.

Reprints and permissions information is available at www.nature.com/reprints.

Publisher's note Springer Nature remains neutral with regard to jurisdictional claims in published maps and institutional affiliations.



Open Access This article is licensed under a Creative Commons Attribution 4.0 International License, which permits use, sharing, adaptation, distribution and reproduction in any medium or format, as long as you give appropriate credit to the original author(s) and the source, provide a link to the Creative Commons licence, and indicate if changes were made. The images or other third party material in this article are included in the article's Creative Commons licence, unless indicated otherwise in a credit line to the material. If material is not included in the article's Creative Commons licence and your intended use is not permitted by statutory regulation or exceeds the permitted use, you will need to obtain permission directly from the copyright holder. To view a copy of this licence, visit <http://creativecommons.org/licenses/by/4.0/>.

© The Author(s) 2022